A Journal of the Gesellschaft Deutscher Chemiker

Angewandte International Edition GDCh Chemie

www.angewandte.org

Accepted Article

Title: Intelligent Solar Water Evaporation

Authors: Liangti Qu, Panpan Zhang, Feng Liu, Qihua Liao, Houze Yao, Hongya Geng, Huhu Cheng, and Chun Li

To be cited as: *Angew. Chem. Int. Ed.* 10.1002/anie.201810345
Angew. Chem. 10.1002/ange.201810345

Link to VoR: http://dx.doi.org/10.1002/anie.201810345
http://dx.doi.org/10.1002/ange.201810345

WILEY-VCH

10.1002/anie.201810345

WILEY-VCH

Intelligent Solar Water Evaporation

Panpan Zhang, Feng Liu, Qihua Liao, Houze Yao, Hongya Geng, Huhu Cheng, Chun Li, Liangti Qu*

Abstract: *The intelligent solar water evaporation (iSWE) is achieved based on the thermally-responsive and microstructured graphene/poly(N-isopropylacrylamide) (mG/PNIPAm) membrane with self-adaptive "on/off" switches under sun. In compliance with the varying solar intensity, mG/PNIPAm membrane exhibits tunable water evaporation through the reversible transformation of microstructures similar to stomatal opening/closing features of leaves. Consequently, this mG/PNIPAm membrane has a high increment of water evaporation rate (ΔWER) of 1.66 kg m^{-2} h^{-1} under weak sunlight (intensity < 1 sun) and a low ΔWER of 0.24 kg m^{-2} h^{-1} under intense sunlight (1 sun < intensity < 2 sun). By designing the double layer structure with predictable shape and dynamics, the leaf-like membrane can further autonomously modulate the water evaporation by self-curling itself under intense solar irradiation in accordance with the simulation results. This mG/PNIPAm provides a smart material platform with self-adapting functions in response to the changeable environments.*

In nature, a variety of plants takes advantage of solar energy and water for the activities of photosynthesis, and equips themselves with self-adaptive functions to survive in the varied environments.[1] Examples for botanical phenomena include the stomatal opening/closing of plant leaves to regulate the water transpiration rate,[2] the cactus leaves degenerating into thorns to adapt to the desert environment,[3] and the leaves of gramineous plants self-curling to reduce water loss at summer noon.[4] All these self-adaptive responses of plants to the changeable environment play an important role to sustain life. Currently, various materials with excellent photothermal conversion ability have been explored for the solar steam generation.[5] However, the development of leaf-like smart material with self-adaptive functions for intelligent solar water evaporation (iSWE) is challenging and not reported yet so far.

Herein, we propose the concept of iSWE based on thermally-responsive and microstructured graphene/poly(N-isopropylacrylamide) (mG/PNIPAm) membrane with self-regulative "on/off" switches driven by sunlight. The synergetic effect of excellent photothermal conversion of graphene and fast thermally responsive feature of PNIPAm allows the mG/PNIPAm membrane with reversible opening/closing microstructures for iSWE, which is similar to stomatal opening/closing features of natural leaves. Adapting to the varying sunlight, the mG/PNIPAm has a high increment of water evaporation rate (ΔWER) of 1.66 kg m^{-2} h^{-1} under weak solar irradiation (intensity < 1 sun), and a low ΔWER of 0.24 kg m^{-2} h^{-1} under intense solar irradiation (1 sun < intensity < 2 sun), respectively. By designing the double-layer leaf or flower structures through laser-processing technology, the intelligent membranes can proactively curl or fold themselves to modulate the water loss under intense sunlight. This work demonstrates iSWE based on mG/PNIPAm membrane and provides a fundamental approach to the development of other intelligent materials with environmental-adaptive functions.

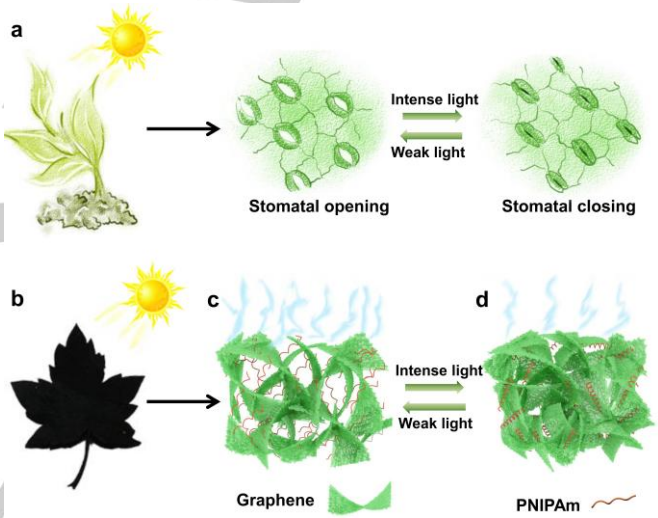

Scheme 1. The concept of iSWE and mechanism illustration. a) Schematic illustration of stomatal opening/closing of leaves under intense and weak sunlight irradiation, respectively. b) A leaf-like mG/PNIPAm membrane. c,d) Under different intensity of solar irradiation, the water transport channels can be autonomously turned on and off by the opening and closing of microstructures.

Stomata are small pores on the surfaces of leaves and stalks, which play an important role to regulate the water transpiration rate of plants. Under weak solar irradiation, the stomata are open to tailor water loss for photosynthesis. However, the stomata become closed under relatively intense solar irradiation to reduce water loss in order to maintain life (Scheme 1a).[6] Inspired by stomatal opening/closing features of plant leaves, we design the iSWE with self-adaptive "on/off" switches for tunable water transport under sunlight. Graphene-based materials with excellent solar absorption ability, outstanding photothermal conversion performance, and easily engineering into artificially networked structure,[7] have been demonstrated for water evaporation.[8] By introducing the thermally-responsive PNIPAm into the microporous graphene framework, which is well known for its reversible phase transitions at its lower critical solution temperature (LCST)

[*] P. Zhang, Q. Liao, H. Yao, Dr. H. Cheng, Prof. L. Qu
Key Laboratory for Advanced Materials Processing Technology, Ministry of Education of China; State Key Laboratory of Tribology, Department of Mechanical Engineering, Tsinghua University, Beijing 100084, PR China.
E-mail: lqu@mail.tsinghua.edu.cn
Prof. F. Liu
State Key Laboratory of Nonlinear Mechanics, Institute of Mechanics, Chinese Academy of Sciences, Beijing 100190, China.
H. Geng, Prof. C. Li, Prof. L. Qu
Department of Chemistry, Tsinghua University, Beijing 100084, PR China.
Prof. L. Qu
School of Chemistry and Chemical Engineering, Beijing Institute of Technology, Beijing 100081, PR China.
E-mail: lqu@bit.edu.cn

(Figure S1),[9] a photothermally responsive mG/PNIPAm membrane is rationally designed for iSWE.

A leaf-like mG/PNIPAm membrane can be easily fabricated through the laser-processing technology (Scheme 1b). Under sunlight, graphene as the solar absorber layer can efficiently convert the solar energy into heat. Below the LCST of mG/PNIPAm under weak solar irradiation (Scheme 1c), the mG/PNIPAm micropores are in an open state, facilitating fast water transport for efficient iSWE. Under intense solar irradiation, the temperature is above the LCST of mG/PNIPAm. The shrink of PNIPAm chains pulls graphene sheets together, and the mG/PNIPAm microstructures are contracted or even blocked, resulting in reduced water evaporation rate (Scheme 1d). Due to the synergetic effect of excellent solar-thermal conversion of graphene and fast thermally-responsive feature of PNIPAm, these water transport channels can be autonomously turned on and off by the opening and closing of microstructures, presenting leaf-like self-adaptive property in compliance with the changeable sunlight intensity.

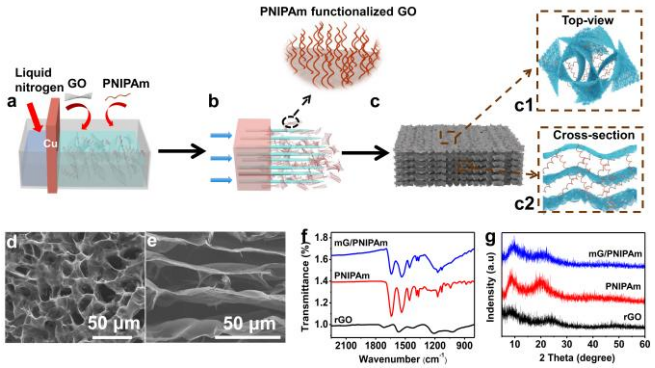

Figure 1. Fabrication and characteristics of mG/PNIPAm membrane. a) Lab-made directional freeze casting container with unidirectional cold source (liquid nitrogen), thermal conductor (copper, Cu) and PNIPAm functionalized graphene oxide (GO) solutions. b) PNIPAm functionalized GO solutions are subjected to directional freeze casting. c) After freeze-drying and reduction under the vapor of hydrazine hydrate, mG/PNIPAm membrane is obtained. c1, c2) Illustration of the top-view and cross-section structures of mG/PNIPAm membrane. d,e) The top-view and cross-section scanning electron microscopy (SEM) images of mG/PNIPAm. f,g) Fourier transform Infrared (FT-IR) spectra and X-ray diffraction (XRD) patterns of rGO, PNIPAm and mG/PNIPAm, respectively.

The mG/PNIPAm is prepared by directionally freezing technique using a lab-made container with unilateral cold source and thermal conductor (Figure 1a and 1b).[8a, 10] After freeze-drying and reduction under the vapor of hydrazine hydrate,[11] the mG/PNIPAm membrane is obtained (Figure 1c). The top view of mG/PNIPAm membrane presents a typical microporous structure with the sizes ranging from 10 to 20 μm (Figure 1c1 and 1d). Owing to the directional growth of ice crystals caused by the unilateral cold source, the assembly of PNIPAm functionalized graphene sheet is solidified in order. As a result, the cross-section shows a well-organized layer-by-layer structure (Figure 1c2 and 1e). The uniform and strong attachment of PNIPAm on the surface of graphene is mainly due to the hydrogen bonding (Figure S2a).[12] mG/PNIPAm exhibits new characteristic peaks at 1642, 1540, and 1367~1460 cm^{-1} compared with reduced graphene oxide (rGO), which belongs to the absorption of PNIPAm (Figure 1f).[13] XRD patterns verify that mG/PNIPAm shows two broad peaks at 7.5° and 22° due to the introduction of PNIPAm (Figure 1g).[9c] The rGO and mG/PNIPAm reduced under the vapor of hydrazine hydrate present high O contents of 19.68% and 22.50%, respectively, which are attributed to the abundant oxygen-containing functional groups (e.g., O–C=O) (Figure S2b and S2c). The C1s X-ray photoelectron spectroscopy (XPS) of mG/PNIPAm shows the new peak of C–N (≈285.4 eV), and the N1s of XPS exhibits the existence of N–H (≈398.8 eV) and N–C=O (≈399.7 eV) (Figure S2d and S2e), resulting in the formation of hydrogen bonding between PNIPAm and graphene.[14] With the pH changes from 4 to 10, the zeta potentials of mG/PNIPAm are much lower than that of original rGO because of the strong coating of PNIPAm on graphene sheets (Figure S2f).[15] All these results demonstrate that PNIPAm is well attached on the surface of graphene sheets.

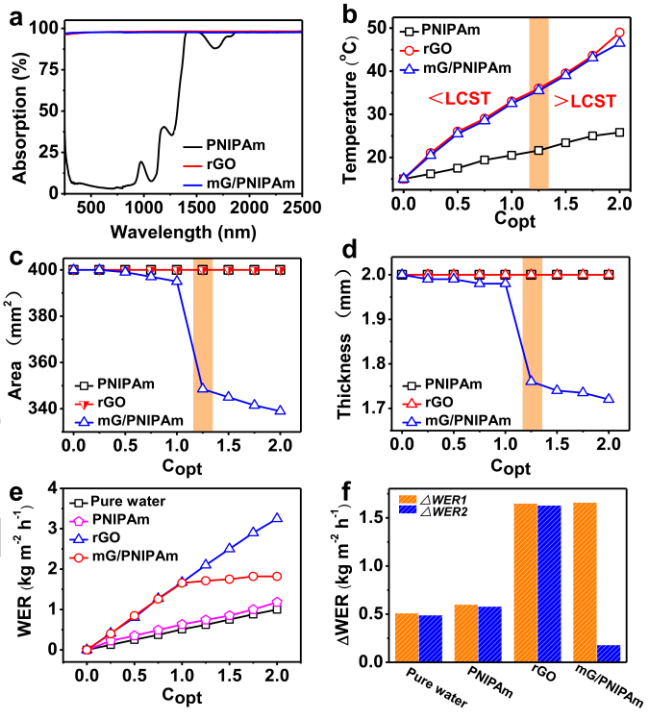

Figure 2. Performance characteristics of the iSWE based on mG/PNIPAm membrane. a) Absorption spectra of PNIPAm, rGO and mG/PNIPAm in the wavelength range of 250–2500 nm. b) Surface temperatures of PNIPAm, rGO and mG/PNIPAm under the solar illumination of 0–2 sun (1 C_{opt}=1 kW m^{-2}=1 sun). c,d) Surface area and thickness variations of PNIPAm, rGO and mG/PNIPAm under different solar illumination (0–2 sun). e) Water evaporation rate (WER) based on pure water, PNIPAm, rGO and mG/PNIPAm under sunlight (0–2 sun). f) The ΔWER of pure water, PNIPAm, rGO and mG/PNIPAm under the solar illumination of 0–2 sun. ΔWER1 is the increment of WER under weak solar illumination (intensity < 1 sun), and ΔWER2 is the increment of WER under strong solar illumination (1 sun < intensity < 2 sun).

In order to understand the stomatal opening/closure behaviors of plant leaves, we put the leaves of epipremnum aureum under natural environment (Figure S3a). The stomatal closure on the leaves is observed when the solar intensity is *ca* 1.2 sun (Figure S3b). Considering the highest solar density under natural environment can reach 1.5 sun, we chose the solar intensity of 0–2 sun to conduct the experiments. The mG/PNIPAm harvests *ca* 99% incident light from 250 to 2500 nm (Figure 2a), and the coating of PNIPAm on graphene sheet has no influence on the excellent solar absorption of graphene. Under the solar illumination of 0–2 sun, the surface temperatures of mG/PNIPAm can quickly increase from 18 to 50 °C, which is

similar with that of original rGO (Figure 2b and Figure S4). For pure PNIPAm, the surface temperatures only change from 18 to 28.6 °C in the same solar illumination range (0–2 sun) because of the poor sunlight absorption, which is below its LCST. As a result, the phase-transition of mG/PNIPAm initiates at the LCST (1.25 sun, *ca* 35 °C) (Figure S5), and obvious surface area and thickness shrinkage of mG/PNIPAm are observed compared with original rGO and PNIPAm (Figure 2c and 2d).

The WERs of rGO and PNIPAm show a linear growth trend with the increased solar intensity (Figure 2e). For mG/PNIPAm, the WER presents linear increase firstly (intensity < 1 sun) and then tends to grow slowly (1 sun < intensity < 2 sun). Under weak solar illumination (intensity < 1 sun), the mG/PNIPAm with open macropores delivers the comparable △WER1 of 1.65 kg m^{-2} h^{-1} with rGO (1.67 kg m^{-2} h^{-1}). When the solar intensity increases from 1 to 2 sun, the phase change of mG/PNIPAm happens and the water transport channels of mG/PNIPAm are turned off. The △WER2 of mG/PNIPAm is 0.24 kg m^{-2} h^{-1}, much lower than that of rGO (1.58 kg m^{-2} h^{-1}), demonstrating that the leaf-like mG/PNIPAm membrane presents similar stomatal closure behavior to reduce water loss under intense sunlight (Figure 2f). Impressively, the WER is completely reversible without obvious decay under the solar illumination of 0.25 and 2 sun for 10 cycles (Figure S6), respectively, verifying that mG/PNIPAm with self-adaptive functions exhibits iSWE in response to the varying sunlight intensity.

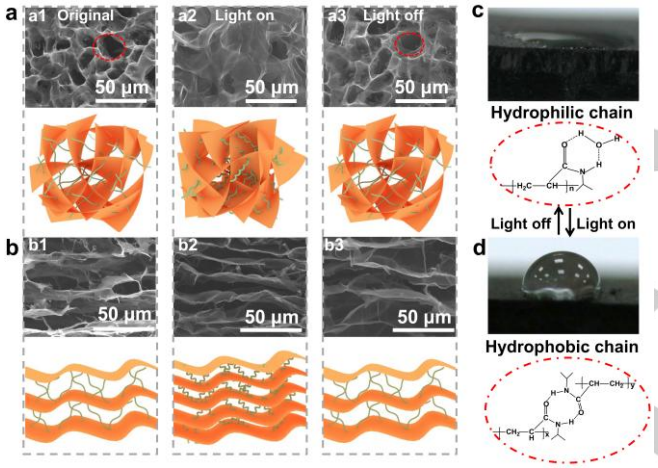

Figure 3. Working mechanism of iSWE. a,b) SEM images and corresponding mechanism illustration of the reversible opening/closing of mG/PNIPAm microstructures (1.5 sun). c,d) The reversible water contact angle (CA) change of mG/PNIPAm (1.5 sun).

Besides, the working mechanism of iSWE based on mG/PNIPAm is explored. The iSWE arises from the unique physicochemical properties of graphene and PNIPAm system, such as the reversible opening/closing of microstructures and switch of hydrophilicity/hydrophobicity. The temperature of original mG/PNIPAm is below its LCST, and the microstructures of mG/PNIPAm are in an open state (Figure 3a1 and 3b1). Benefiting from the exposure of hydrophilic chain in PNIPAm, mG/PNIPAm exhibits hydrophilic property with the water CA of 0° (Figure 3c), facilitating fast water transport through the open pores. Under intense solar illumination (1.5 sun), the phase change of PNIPAm is initiated, the spring coefficient and equilibrium distance in the molecular dynamics (MD) simulation changes from 0 pg·μs^{-2} and 2 μm to 37,555 pg·μs^{-2} and 0.6 μm, respectively (see detailed simulation process; Figure S7 and S8).[16] The shrinkage of PNIPAm chains causes the bending of graphene sheets and pulls the graphene sheets together. Consequently, the pores in mG/PNIPAm microstructures are contracted or even blocked, and the lamellar spaces of the graphene sheets are obviously reduced (Figure 3a2 and 3b2). Meantime, PNIPAm breaks its hydrogen bonds with water molecules instead of exposing more hydrophobic chains, leading to the CA of mG/PNIPAm increase to 90 ° (Figure 3d).[9a, 17] The closed microstructures together with increased CA of mG/PNIPAm efficiently hinder the transport of water molecules, slowing the water evaporation under intense sunlight. Besides, the opening/closing feature of microstructures and switch of hydrophilicity/hydrophobicity based on mG/PNIPAm at the LCST is fully reversible (Figure 3a3 and 3b3).

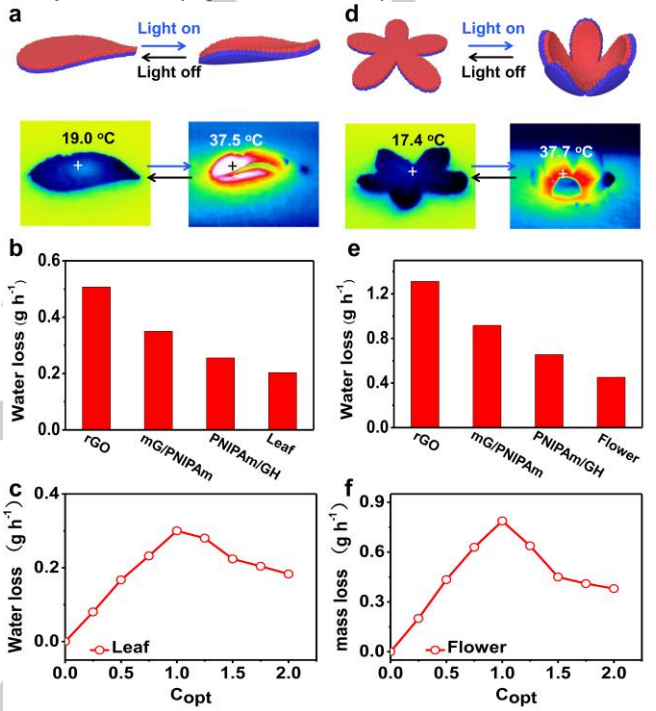

Figure 4. Performance characteristics of the leaf and flower structures with self-adaptive ability. a) The MD simulation results and Infrared (IR) images of the reversible self-curling process of the leaf (1.5 sun). b) Mass loss of water based on rGO, mG/PNIPAm, PNIPAm/GH and leaf with the same shape and size (S=2 cm^2) under 1.5 sun. c) Mass loss of the self-curling leaf under the solar illumination of 0–2 sun. d) The MD simulation results and IR images of the reversible self-folding process of the flower (1.5 sun). e) Mass loss of water based on rGO, mG/PNIPAm, PNIPAm/GH and flower with the same shape and size (S=5.25 cm^2) under 1.5 sun. f) Mass loss of the self-folding flower under the solar illumination of 0–2 sun.

To further reduce water loss adapting to the intense solar irradiation, we designed a double layer membrane with self-curling ability similar to the plants, in which the upper layer is the crosslinked PNIPAm/graphene hydrogel (PNIPAm/GH) and the bottom layer is mG/PNIPAm (Figure S9), endowing the two layers with different swelling/shrinking properties. In the simulation, the coarse grain progressing is conducted to simulate the double layer membrane for the self-curling

properties, and a face center cubic (FCC) structured beads are assumed. The simulation results show that the bond lengths for upper (PNIPAm/GH) and bottom layers (mG/PNIPAm) are reduced by 15% and 7% similar to the observation in the experiments (Figure S10). Meantime, the Young's modulus of PNIPAm/GH and mG/PNIPAm enhance from 86.2 and 75.8 MPa (original) to 500 and 300 MPa (1.5 sun), respectively. These simulation results show the well-defined self-curling morphology of the leaf and self-folding phenomena of the flower structure for efficient iSWE (Figure S11 and S12).

By varying the light intensity from 0 to 1.5 sun, we observed that the leaf tends to self-curl within 5 min with the bending angle of *ca* 60^o (Figure S13a and S14a), leading to the sunlight receiving area reduce from 2.0 to 1.27 cm^2 (Figure 4a). The water loss of leaf is 0.20 g h^{-1}, 2.5, 1.75, 1.28 times lower than that of pure rGO, mG/PNIPAm and PNIPAm/GH (Figure 4b), respectively. The closed water transport channels and the leaf's self-curling work together to tailor the water evaporation according to the varying sunlight density. Under the solar illumination of 0–2 sun, the leaf structure presents the midday depression phenomenon of plant, delivering a high water loss of 0.3 g h^{-1} under 1 sun and a low water loss of 0.18 g h^{-1} under 2 sun (Figure 4c). For the flower structure, its five free petals toward the center and undergo from an open to a closed state within 10 min (1.5 sun) with the bending angle of *ca* 90^o (Figure 4d, Figure S13b and S14b), causing the decrease of sunlight receiving area from 5.25 to 2.6 cm^2. The water loss of flower shape is 0.45 g h^{-1} under a folding state, 2.9, 2.04 and 1.46 times lower than that of pure rGO, mG/PNIPAm and PNIPAm/GH (Figure 4e), respectively. Benefiting from the closed pores and petal's self-folding, the flower shows a much lower water loss of 0.38 g h^{-1} under 2 sun compared with the water loss under 1 sun (0.79 g h^{-1}) (Figure 4f). Therefore, by rationally designing the smart membrane with predictable shapes and dynamics, this double layer structures can autonomously curl or fold themselves to further reduce the WER under intense sunlight, demonstrating the feasibility of the intelligent materials with self-adaptive ability in response to changeable environment.

In summary, a leaf-like mG/PNIPAm membrane with self-adaptive functions has been demonstrated for efficient iSWE. Adapting to the varying sunlight, mG/PNIPAm presents tunable WER through turning on and off the water transport channels, exhibiting similar stomatal opening/closing features of leaves. Consequently, the mG/PNIPAm membrane endows fast water evaporation through the open macropores with a high ΔWER under the weak sunlight (intensity < 1 sun), and a low ΔWER under the intense sunlight (1 sun < intensity < 2 sun) because of the closure of macrostructures. Moreover, by designing the double layer structure with leaf and flower structures, the intelligent membranes can proactively curl or fold themselves to further tailor the WER under intense sunlight. This leaf-like mG/PNIPAm opens significant opportunities to the development of intelligent materials with environmental-adaptive functions of significant importance.

Acknowledgements

The authors declare no competing financial interest. We acknowledge the financial support from the Ministry of Science and Technology of China (2017YFB1104300, 2016YFA0200200), NSFC (No. 51673026, 51433005, 21674056), NSFC-MAECI (51861135202), Beijing Natural Science Foundation (2152028), Beijing Municipal Science and Technology Commission (Z161100002116022, Z161100002116029). National Natural Science Foundation of China (No. 11602272, 11790292). The Strategic Priority Research Program of the Chinese Academy of Sciences (No. XDB22040503).

Keywords: leaf-like membrane · opening/closing features · intelligent · solar water evaporation · self-adaptive functions

[1] a) I. Baxter, B. P. Dilkes, *Science* **2012**, *336*, 1661–1663; b) U. Berger, C. Piou, K. Schiffers, V. Grimm, *Perspect. Plant. Ecol.* **2008**, *9*, 121–135; c) A. B. Nicotra, O. K. Atkin, S. P. Bonser, A. M. Davidson, E. J. Finnegan, U. Mathesius, P. Poot, M. D. Purugganan, C. L. Richards, F. Valladares, M. van Kleunen, *Trends Plant. Sci.* **2010**, *15*, 684–692; d) L. Santamaria, *Acta. Oecol.* **2002**, *23*, 137–154.

[2] a) E. I. Lammertsma, H. J. de Boer, S. C. Dekker, D. L. Dilcher, A. F. Lotter, F. Wagner-Cremer, *PNAS* **2011**, *108*, 4035–4040; b) P. J. Franks, G. D. Farquhar, *Plant Physiol.* **2007**, *143*, 78–87; c) A. M. Hetherington, F. I. Woodward, *Nature* **2003**, *424*, 901–908; d) T. N. Buckley, *New Phytol.* **2005**, *168*, 275–291.

[3] a) N. H. Boke, *Bioscience* **1980**, *30*, 605–610; b) P. Ranjan, J. K. Ranjan, R. L. Misra, M. Dutta, B. Singh, *Genet. Resour. Crop. Ev.* **2016**, *63*, 901–917.

[4] a) B. J. Forde, K. J. Mitchell, E. A. Edge, *Aust. J. Plant Physiol.* **1977**, *4*, 889–899; b) J. L. Liu, P. C. Zuo, J. Sun, D. Lan, *Int. J. Mech. Eng. Educ.* **2015**, *43*, 110–117.

[5] a) M. Zhu, Y. Li, F. Chen, X. Zhu, J. Dai, Y. Li, Z. Yang, X. Yan, J. Song, Y. Wang, E. Hitz, W. Luo, M. Lu, B. Yang, L. Hu, *Adv. Energy Mater.* **2018**, *8*, 1701028; b) N. Xu, X. Hu, W. Xu, X. Li, L. Zhou, S. Zhu, J. Zhu, *Adv. Mater.* **2017**, *29*, 1606762; c) L. Cui, P. Zhang, Y. Xiao, Y. Liang, H. Liang, Z. Cheng, L. Qu, *Adv. Mater.* **2018**, *30*, 1706805; d) F. Zhao, X. Zhou, Y. Shi, X. Qian, M. Alexander, X. Zhao, S. Mendez, R. Yang, L. Qu, G. Yu, *Nat. Nanotechnol.* **2018**, *13*, 489–495; e) R. Li, L. Zhang, L. Shi, P. Wang, *ACS Nano* **2017**, *11*, 3752–3759; f) L. Zhu, M. Gao, C. K. N. Peh, X. Wang, G. W. Ho, *Adv. Energy Mater.* **2018**, *8*, 1702149; g) G. Ni, G. Li, Svetlana V. Boriskina, H. Li, W. Yang, T. Zhang, G. Chen, *Nat. Energy* **2016**, *1*, 16126.

[6] a) H. Ledford, *Nature* **2017**, *546*, 585–586; b) M. R. Carins Murphy, G. J. Jordan, T. J. Brodribb, *Plant Cell Environ.* **2014**, *37*, 124–131; c) N. Martin StPaul, S. Delzon, H. Cochard, *Ecol. Lett.* **2017**, *20*, 1437–1447; d) A. Gargava, C. Arya, S. R. Raghavan, *ACS Appl. Mater. Inter.* **2016**, *8*, 18430–18438;

[7] a) C. G. Hu, J. L. Xue, L. Y. Dong, Y. Jiang, X. P. Wang, L. T. Qu, L. M. Dai, *ACS Nano* **2016**, *10*, 1325–1332; b) L. X. Lv, P. P. Zhang, H. H. Cheng, Y. Zhao, Z. P. Zhang, G. Q. Shi, L. T. Qu, *Small* **2016**, *12*, 3229–3234; c) P. P. Zhang, L. X. Lv, Y. Liang, J. Li, H. Cheng, Y. Zhao, L. T. Qu, *J. Mater. Chem. A* **2016**, *4*, 10118–10123; d) B. W. Yao, J. Chen, L. Huang, Q. Q. Zhou, G. Q. Shi, *Adv. Mater.* **2016**, *28*, 1623–1629.

[8] a) P. P. Zhang, J. Li, L. X. Lv, Y. Zhao, L. T. Qu, *ACS Nano* **2017**, *11*, 5087–5093; b) Y. J. Li, T. T. Gao, Z. Yang, C. J. Chen, W. Luo, J. W. Song, E. Hitz, C. Jia, Y. B. Zhou, B. Y. Liu, B. Yang, L. B. Hu, *Adv. Mater.* **2017**, *29*, 1700981; c) Y. Ito, Y. Tanabe, J. Han, T. Fujita, K. Tanigaki, M. Chen, *Adv. Mater.* **2015**, *27*, 4302–4307; d) H. Ren, M. Tang, B. Guan, K. Wang, J. Yang, F. Wang, M. Wang, J. Shan, Z. Chen, D. Wei, H. Peng, Z. Liu, *Adv. Mater.* **2017**, *29*, 1702590; e) X. Li, W. Xu, M. Tang, L. Zhou, B. Zhu, S. Zhu, J. Zhu, *PNAS* **2016**, *113*,

13953–13958; f) Q. Jiang, L. Tian, K. K. Liu, S. Tadepalli, R. Raliya, P. Biswas, R. R. Naik, S. Singamaneni, *Adv. Mater.* **2016**, *28*, 9400–9407.

[9] a) C. Ma, Y. Shi, D. A. Pena, L. Peng, G. Yu, *Angew Chem Int. Edit.* **2015**, *54*, 7376–7380; b) C. L. Zhang, F. H. Cao, J. L. Wang, Z. L. Yu, J. Ge, Y. Lu, Z. H. Wang, S. H. Yu, *ACS Appl. Mater. Inter.* **2017**, *9*, 24857–24863; c) C. H. Zhu, Y. Lu, J. Peng, J. F. Chen, S. H. Yu, *Adv. Funct. Mater.* **2012**, *22*, 4017–4022; d) C. Teng, J. Qiao, J. Wang, L. Jiang, Y. Zhu, *ACS Nano* **2016**, *10*, 413–420.

[10] F. Zhao, L. Wang, Y. Zhao, L. Qu, L. Dai, *Adv. Mater.* **2017**, *29*, 1604972.

[11] a) P. G. Ren, D. X. Yan, X. Ji, T. Chen, Z. M. Li, *Nanotech.* **2011**, *22*, 055705; b) Z. Q. Niu, J. Chen, H. H. Hng, J. Ma, X. D. Chen, *Adv. Mater.* **2012**, *24*, 4144–4150.

[12] D. Y. Lee, S. Yoon, Y. J. Oh, S. Y. Park, I. In, *Macromol. Chem. and Phys*. **2011**, 212, 336–341.

[13] W. A. Xu, Z. Qin, C. T. Chen, H. R. Kwag, Q. L. Ma, A. Sarkar, M. J. Buehler, D. H. Gracias, *Sci. Adv.* **2017**, *3*, e1701084.

[14] J. C. Liu, N. Wang, L. J. Yu, A. Karton, W. Li, W. X. Zhang, F. Y. Guo, L. L. Hou, Q. F. Cheng, L. Jiang, D. A. Weitz, Y. Zhao, *Nat. Commun.* **2017**, 8, 2011.

[15] L. Huang, J. Chen, T. T. Gao, M. Zhang, Y. R. Li, L. M. Dai, L. T. Qu, G. Q. Shi, *Adv. Mater.* **2016**, 28, 8669–8674.

[16] a) S. Plimpton, *J. Comput. Phys*. **1995**, 117, 1–19; b) A. Stukowski, *Model. Simul. Mater. Sc.* **2009**, 18, 015012;

[17] a) Y. H. Zhao, Y. Wu, L. Wang, M. M. Zhang, X. Chen, M. J. Liu, J. Fan, J. Q. Liu, F. Zhou, Z. K. Wang, *Nat. Commun.* **2017**, *8*; b) Y. Shi, C. B. Ma, L. L. Peng, G. H. Yu, *Adv. Funct. Mater.* **2015**, *25*, 1219–1225.

10.1002/anie.201810345

WILEY-VCH

COMMUNICATION

The intelligient solar water evaporation has been demonstrated based on thermally-responsive and microstructured graphene/poly(N-isopropylacrylamide) (mG/PNIPAm) membrane with self-adaptive functions. In response to the varying sunlight, this leaf-like mG/PNIPAm membrane presents tunable water evaporation rate through turning on and off the water transport channels similar to stomatal opening/closing features

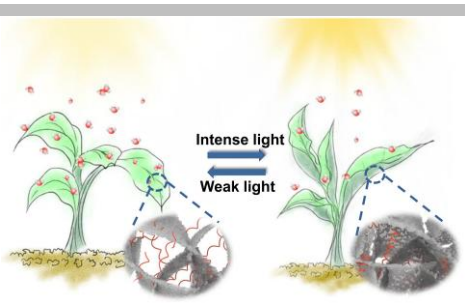

*Panpan Zhang, Feng Liu, Qihua Liao, Houze Yao, Hongya Geng, Huhu Cheng, Chun Li, Liangti Qu**

Intelligent Solar Water Evaporation